ISSN PRINT 2319 1775 Online 2320 7876

Research paper UGC CARE Listed (Group -I) Journal Volume 11, Iss 11, Nov 2022

Effect Of Unsteady MHD Nanofluid In An Asymmetric Wavy Channel With Soret Effect

Prathiba. S.R [1)], Karthika. A[2)]

1) Shrimathi Devkunvar Nanalal Bhatt Vaishnav College for Women, Chennai,, India
2)Sri Krishna College of Engineering and Technology, Coimbatore, India

Abstract

Flow through asymmetric wavy channel is important in electronics coolant in industry and biomedical industry. Numerous investigations have been reported presenting analytical and numerical solutions for a plethora of different geometrical scenarios, such flows are important in rocket propulsion control, crystal growth technology, astrophysical plasma fluid dynamics, tri-biological regulation in moving machine parts and magnetohydrodynamic energy generators. An electrically conducting oscillatory incompressible nanofluid past a asymmetric wavy channel bounded by a porous medium is considered. Appropriate boundary conditions are considered on the boundary of the wavy channel. The nano fluid effects in velocity profile, temperature profile and concentration profile for various parameters are plotted with graphs. Heat and mass transfer effects are analyzed.

1 Introduction

The effects in a wavy wall channel using forced convection was studied by Wang and Chen [12]. Oscillatory flow in an asymmetric wavy channel with magnetic effect was discussed by Sudharsan Reddy *et al.* [11]. The same work in irregular channel with chemical reaction was analyzed by Satya Narayana *et al.* [10]. Soret effect for a wavy channel was discussed by Sasikumar *et al*.[9]. Magnetohydrodynamic flow in rotating systems continues to stimulate significant research in the fields of engineering science and applied mathematics.

Dragon and Grotberg [3] studied the mass transport in a flexible tube with oscillatory flow in the year 1991. Oscillatory Stokes flow in porous media was discussed by Chapman and Higdon [1]. Many studies were gone through the field of oscillatory flow through porous media in the year 2000. Later, Graham and Higdon [4] worked on the oscillatory forcing of flow through porous media. Looker and Carnie [7] discussed the hydrodynamics of an oscillating porous sphere. An exact solution of oscillatory flow through a porous medium in sphere was discussed by Loganathan and Prathiba[5],[6]. Magnetohydrodynamic flow past a rotating cylinder was derived by Prathiba *et al*. [8]. Axial dispersion in packed beds of spheres was done by Crittenden *et al*. [2].

Oscillatory flow through many objects has gained importance lately since it is used in industry and geophysical applications. With a vast array of potential applications, it is fairly evident that a lot of people have put in their minds and thoughts, trying to invent more innovations in this prevalent field. Nano particles have introduced to increase the transfer of heat in the fluid. Many methods are used to progress current of the fluids by dangling nano particles in waters.

Recently the flow of fluids in an asymmetric porous wavy channel was studied by many researchers. In this paper the heat and mass transfer, soret effect on magnetohydrodynamic

ISSN PRINT 2319 1775 Online 2320 7876

Research paper UGC CARE Listed (Group -I) Journal Volume 11, Iss 11, Nov 2022

oscillatory flow of nanofluid through porous medium in asymmetric wavy channel is analysed. The nanofluid effects in velocity contour, temperature profile and concentration profile for various parameters are discoursed. Heat and mass transfer of several parameters are analysed.

2 Governing equations of the problem

Consider the electrically conducting nano fluid with the viscous incompressible flow in a asymmetric wavy channel bounded by the permeable medium.

The wall surface is defined as

$$H_L = d_1 + a_1 cos\left[\frac{2\pi}{\lambda}(x)\right] \tag{1}$$

$$H_R = -d_2 - a_2 cos\left[\frac{2\pi}{\lambda}(x) + \phi\right] \tag{2}$$

where a_1 and a_2 are the amplitude of the left and right of the walls and , d_1 and d_2 are the half width of the channel, λ is the wave length , ϕ is the phase difference, ϕ varies from 0 to π and also have the relation

$$a_1^2 + a_1^2 + 2a_1 a_2 \cos(\phi) \leq (d_1 + d_2) \tag{3}$$

T_1 and T_2 are the temperature of the two walls. Magnetic field is applied normal to the walls.

The governing equation of the nanofluid flow are given by

$$\rho_{nf}\left(\frac{\partial u}{\partial t}\right) = -\frac{\partial p}{\partial x} + \mu_{nf}\frac{\partial^2 u}{\partial y^2} - \sigma B_0^2 u - \frac{\mu_{nf}}{K}u + (\rho\beta_T)_{nf} g(T - T_2) + (\rho\beta_C)_{nf} g(C - C_2) \tag{4}$$

$$\left(\rho C_p\right)_{nf}\frac{\partial T}{\partial t} = K_{nf}\frac{\partial^2 T}{\partial y^2} - \frac{\partial q}{\partial y} + Q^*(T - T_2) \tag{5}$$

$$\frac{\partial C}{\partial t} = D\frac{\partial^2 C}{\partial y^2} - K_r^*(C - C_2) + \frac{DK_T}{T_m}\frac{\partial^2 T}{\partial y^2} \tag{6}$$

where u - velocity component along x axis. ρ_{nf} - nanofluid density , μ_{nf} - nanofluid viscosity , σ - electric conductivity of the fluid, B_0 - uniform magnetic field, g - acceleration due to gravity, $(\beta_T)_{nf}$ - coefficient of thermal expansion of nanofluid, $(\beta_C)_{nf}$ - coefficient of mass expansion of nanofluid, T - temperature of the nanofluid, T_0 - temperature , C - concentration of the nanofluid, C_0 - concentration, $\left(\rho C_p\right)_{nf}$ - heat capacity of the nanofluid, k - permeable parameter, q - radiative heat flux, K_r^* - chemical reaction parameter, Q^* - heat source parameter and D - mass diffusion coefficient.

Hamilton and Crosser defined the effective properties of the nanofluid as

$$\rho_{nf} = (1 - \emptyset)\rho_f + \emptyset\rho_s \tag{7}$$

$$(\rho\beta)_{nf} = (1 - \emptyset)(\rho\beta)_f + \emptyset(\rho\beta)_s \tag{8}$$

$$(\rho C_p)_{nf} = (1 - \emptyset)\left(\rho C_p\right)_f + \emptyset(\rho C_p)_s \tag{9}$$

$$\mu_{nf} = \frac{\mu_f}{(1-\emptyset)^{2.5}} \tag{10}$$

ISSN PRINT 2319 1775 Online 2320 7876

Research paper UGC CARE Listed (Group -I) Journal Volume 11, Iss 11, Nov 2022

$$K_{nf} = K_f \left(\frac{K_s + 2K_f - 2\emptyset(K_f - K_f)}{K_s + 2K_f + 2\emptyset(K_f - K_f)} \right) \tag{11}$$

$$\alpha_{nf} = \frac{K_{nf}}{(\rho C_p)_{nf}} \tag{12}$$

where ρ_s and ρ_f are the solid and fluid particles densities of the respectively. β_s and β_f are the solid and fluid coefficients of thermal expansion respectively. α_{nf} - thermal diffusivity. K_f and K_s - base fluid and solid conductivities respectively. $\emptyset$ is the solid volume fraction of nanofluid.

The heat flux and the pressure gradient be

$$\frac{\partial q}{\partial y} = 4\alpha^2(T_2 - T) \tag{13}$$

$$-\frac{\partial P}{\partial x} = \lambda e^{int'} \tag{14}$$

where α - mean radio activity absorption coefficient and n - frequency of oscillation.

Boundary conditions are

$$y = H_L : u = 0, T = T_1, C = C_1 \tag{15}$$

$$y = H_R : u = 0, T = T_2, C = C_2 \tag{16}$$

The non dimensional quantities are

$$u' = \frac{u}{U}, x' = \frac{x}{\lambda}, \quad y' = \frac{y}{d}, \quad a = \frac{a_1}{d_1}, b = \frac{b_1}{d_1}, d = \frac{d_2}{d_1}, H_L = \frac{h_1}{d_1}, H_R = \frac{h_2}{d_1}, \quad t' = \frac{Ut}{d}$$

$$s^2 = \frac{1}{D_a}, \quad D_a = \frac{K_f}{d^2}, Q = \frac{Q^* d^2}{K_f}, K_r = \frac{dK_r^*}{U}, S_r = \frac{DK_T}{T_m dU} \frac{(T_1 - T_2)}{(C_1 - C_2)}, \quad M^2 = \frac{\sigma {B_0}^2 d^2}{\mu_f},$$

$$G_r = \frac{g(\beta_T)_f d^2 (T_1 - T_2)}{\nu_f U}, \quad G_c = \frac{g(\beta_c)_f d^2 (C_1 - C_2)}{\nu_f U}, \quad p' = \frac{p d^2}{\mu_f \lambda U}, \quad P_e = \frac{Ud(\rho C_p)_{nf}}{K}$$

$$S_c = \frac{D}{Ud}, R_e = \frac{Ud}{\nu_f}, N^2 = \frac{4\alpha^2 d^2}{K}, \quad \theta = \frac{(T - T_2)}{(T_1 - T_2)}, \phi = \frac{(C - C_2)}{(C_1 - C_2)} \tag{17}$$

where U is the mean flow velocity, G_r is Grashof number, G_m is modified Grashof number, R_e is the Reynolds number, P_e is the Peclet number, D_a is the Darcy number, S_r is Soret number, Q is heat source, K_r chemical reaction parameter, N is radiation parameter and S_c is Schmidt number.

Using the non dimensional terms

$$R_e \frac{\partial u'}{\partial t} = \lambda e^{int'} + \frac{\partial^2 u'}{\partial y'^2} + + G_r\theta + G_C\phi - (s^2 + M^2)u' \tag{18}$$

$$P_e \frac{\partial \theta}{\partial t'} = \frac{\partial^2 \theta}{\partial y'^2} + (N^2 + Q)\theta \tag{19}$$

$$\frac{\partial \phi}{\partial t'} = S_c \frac{\partial^2 \phi}{\partial y'^2} - K_r\phi - S_r \frac{\partial^2 \theta}{\partial y'^2} \tag{20}$$

The corresponding non dimensional boundary conditions are

ISSN PRINT 2319 1775 Online 2320 7876

Research paper UGC CARE Listed (Group -I) Journal Volume 11, Iss 11, Nov 2022

$$u' = 0, \theta = 1, \phi = 1 \quad \text{at } y' = h_1 \tag{21}$$

$$u' = 0, \theta = 0, \phi = 0 \quad \text{at } y' = h_2 \tag{22}$$

3 Solution of the Problem

For solving the equations, assume that

$$u(y', t') = u_0(y')e^{int'} \tag{23}$$

$$\theta(y', t') = \theta_0(y')e^{int'} \tag{24}$$

$$\phi(y', t') = \phi_0(y')e^{int'} \tag{25}$$

Now substituting equations (23) - (25) in equations (18)-(20)

$$\frac{d^2u_0}{dy'^2} - (R_e in + M^2 + s^2)u_0 = -(G_r\theta_0 + G_C\phi_0 - \lambda) \tag{26}$$

$$\frac{d^2\theta_0}{dy'^2} + (N^2 + Q - P_e in)\theta_0 = 0 \tag{27}$$

$$S_c\frac{d^2\phi_0}{dy'^2} + S_r\frac{d^2\theta_0}{dy'^2} - (K_r + in)\phi_0 = 0 \tag{28}$$

Substituting equation (27) in equation (28), then equation (28) becomes

$$\frac{d^2\phi_0}{dy'^2} + \frac{S_r}{S_c}(N^2 + Q - P_e in)\theta_0 - \frac{(K_r+in)}{S_c}\phi_0 = 0 \tag{29}$$

And the boundary conditions are

$$u_0 = 0, \theta_0 = 1, \phi_0 = 1 \quad \text{at } y = h_1 \tag{30}$$

$$u_0 = 0, \theta_0 = 0, \phi_0 = 0 \quad \text{at } y = h_2 \tag{31}$$

Solving equations (26),(27) and (29) along with the boundary conditions (30) and (31), then

$$u_0 = A_3e^{E_3y'} + A_4e^{-E_3y'} - \frac{1}{{E_3}^2}(\lambda - G_r\theta_0 - G_c\varphi_0) \tag{32}$$

$$\theta_0 = \frac{sin\ E_1(h_2 - y')}{\sin E_1(h_2 - h_1)} \tag{33}$$

$$\varphi_0 = A_1e^{E_2y'} + A_2e^{-E_2y'} + \left(\frac{S_r}{S_c}\right)\left(\frac{{E_1}^2}{{E_2}^2}\right)\theta_0 \tag{34}$$

Using equations (23) –(25), then equations (32)-(34) becomes

$$u = \left[A_3e^{E_3y'} + A_4e^{-E_3y'} - \left(\frac{\lambda}{{E_3}^2}\right) + \left(\frac{G_r}{{E_3}^2}\right)\left(\frac{sin\ E_1(h_2 - y')}{\sin E_1(h_2 - h_1)}\right) - \left(\frac{G_c}{{E_3}^2}\right)\left(A_1e^{E_2y'} + A_2e^{-E_2y'} + \left(\frac{S_r}{S_c}\right)\left(\frac{{E_1}^2}{{E_2}^2}\right)\left(\frac{sin\ E_1(h_2 - y')}{\sin E_1(h_2 - h_1)}\right)\right)\right]e^{int'} \tag{35}$$

$$\theta = \left[\frac{sin\ E_1(h_2 - y')}{\sin E_1(h_2 - h_1)}\right]e^{int'} \tag{36}$$

ISSN PRINT 2319 1775 Online 2320 7876

Research paper UGC CARE Listed (Group -I) Journal Volume 11, Iss 11, Nov 2022

$$\phi = \left[A_1 e^{E_2 y'} + A_2 e^{-E_2 y'} + \left(\frac{S_r}{S_c}\right)\left(\frac{{E_1}^2}{{E_2}^2}\right)\left(\frac{\sin E_1(h_2 - y')}{\sin E_1(h_2 - h_1)}\right)\right] e^{int'} \quad (37)$$

4 Shear Stress

The shear stress is

$$\tau = -\mu \left(\frac{\partial u}{\partial y'}\right)_{y=h_1,h_2}$$

$$\tau = -\mu \left[\left[A_3 e^{E_3 y'} E_3 - A_4 e^{-E_3 y'} E_3 - E_1 \left(\frac{G_r}{{E_3}^2}\right)\left(\frac{\cos E_1(h_2 - y')}{\sin E_1(h_2 - h_1)}\right) - \left(\frac{G_c}{{E_3}^2}\right)\left(A_1 e^{E_2 y'} E_2 - A_2 e^{-E_2 y'} E_2 - E_1 \left(\frac{S_r}{S_c}\right)\left(\frac{{E_1}^2}{{E_2}^2}\right)\left(\frac{\cos E_1(h_2 - y')}{\sin E_1(h_2 - h_1)}\right)\right)\right] e^{int'}\right]_{y=h_1,h_2} \quad (38)$$

5 Heat Transfer

The rate of heat transfer

$$Nu = -\left[\frac{\partial \theta}{\partial y'}\right]_{y'=h_1,h_2}$$

$$Nu = E_1 \left[\left[\frac{\cos E_1(h_2 - y')}{\sin E_1(h_1 - h_2)}\right] e^{int'}\right]_{y'=h_1,h_2} \quad (39)$$

6 Mass Transfer

The rate of mass transfer

$$Sh = -\left[\frac{\partial \phi}{\partial y'}\right]_{y'=h_1,h_2}$$

$$Sh = \left[\left[A_2 e^{-E_2 y'} E_2 - A_1 e^{E_2 y'} E_2 + E_1 \left(\frac{S_r}{S_c}\right)\left(\frac{{E_1}^2}{{E_2}^2}\right)\left(\frac{\cos E_1(h_2 - y')}{\sin E_1(h_2 - h_1)}\right)\right] e^{int'}\right]_{y'=h_1,h_2} \quad (40)$$

7 Results and Discussion

The various parameter of the nanofluid past asymmetric wavy channel is discussed. The velocity profile for various parameters are studied using different values. The results are obtained for the flows by using the Fig.1 to Fig.21.

Velocity profiles are exposed in Fig.3.1 to Fig.3.8. In Fig.1 velocity declines for growing values of the parameter Gc and with the remaining parameters are M=1, N=2, Q=2, Sc=0.6, Re=1, λ=1, Pe=0.1, Gr=2, Sr=1 and s=1. From Fig.2, it is realized that the velocity gradually declines with growing Schmidt number with the remaining parameters M=1, N=2, Q=2, Gc=1, , Re=1, λ=1, Pe=0.1, Gr=2, Sr=1 and s=1. For increasing N the velocity becomes increases steadily. These results are existing in fig.3 and the lasting parameters are parameters M=1, Q=2, Gc=1, Re=1, λ=1, Pe=0.1, Gr=2, Sr=1 and s=1. For increasing magnetic parameter M the velocity becomes declines. These results are present in fig.4 and the remaining parameters are same in the previous figure.

ISSN PRINT 2319 1775 Online 2320 7876

Research paper UGC CARE Listed (Group -I) Journal Volume 11, Iss 11, Nov 2022

For increasing Pe the velocity becomes increases for some radius , after certain period it is gradually decreasing. These results are present in fig.5 and the remaining parameters are same in the previous figure. The behaviour of Grashof number in velocity profile is noticeable. Velocity increases for Grashof number and the variation are large. That is shown in Fig.6. When a graph is plotted between velocity and radial distance of the wavy channel , (Fig.7) velocity rises with increase Soret number. Fig.8 represents velocity profile for several values of the permeability. Here velocity profile intensifications with increasing Q and the remaining parameters are Pe=0.1, Gc=1, Sc=0.6, Re=1, Gr=2, N=2, Sr=1.

Temperature profiles are represented in Fig.9 to Fig.14. From Fig.9, we see that there is no noteworthy change for different values of Gc. Temperature decreases for increasing Peclet number and the rate of decrement is in Fig.10. Then for higher y, a slight slope is in the Peclet number, just like the one seen in Fig.8. For negative values of Q temperature declines for reducing values of heat source and the remaining parameters are Pe=0.1, Gc=1, Sc=0.3, Re=1, Gr=2, N=2, Sr=1 that is in Fig.11.If a graph is designed against temperature to N (Fig.12) in the occurrence of a permeability and magnetic parameter, the increase rate of N leads to the temperature to decrease. In Fig.13. temperature diminutions for growing numbers of positive Q, with Pe=0.1, Gc=1, Sc=0.3, Re=1, Gr=2, N=2, Sr=1. Temperature decreases as the values of *x* magnetic parameter rises and x reaches a single value for some y is presented in Fig.14.

Concentration profile is studied from Fig.15 to Fig.19. In Fig.15 concentration is decreases and tends to a single value for different increasing value of the frequency parameter. If Sc is increases, the concentration profile mostly upsurges with rising y, then for higher Sc, a small slump is initiate in concentration profile, as seen in Fig.16. The behaviour of concentration profile is slightly different for various values of Q. It gradually decreases for increasing values of Q is shown in Fig.17. Again, for the varying Peclet values, concentration decreases and suddenly raises for higher y, reaches a single value for some y, as represented in Fig.18. And, for the varying Soret values, concentration increases, for higher values the raise in concentration profile is very high and suddenly reduced to some common value, as represented in Fig.19.

Shear stress is represented in Fig.20 and Fig.21. As seen in Fig.20, shear stress declines as the Schmidt number rises with Pe=0.3, Gc=1, Q=2, Re=1, Gr=2, N=2, Sr=1. Once a chart is designed for different values of Peclet number (Fig.21), initially skin friction increases for increasing Peclet number but for higher values of y it decreases.

The rate of heat transfer is denoted in Fig.22 and Fig.23. As understood in Fig.22, heat transfer raises as the radiation parameter upsurges with Pe=0.3, Gc=1, Q=2, Re=1, Gr=2, Sc=0.6, Sr=1. For various values of Q (Fig.23), heat transfer decreases and differences are very clear with very small N and the remaining values are Pe=0.3, Gc=1, N=0.1, Re=1, Gr=2, Sc=0.6, Sr=1. Fig.24 is for mass transfer with different Schmidt number. When ever the Schmidt number upsurges the mass transfer rises gradually.

ISSN PRINT 2319 1775 Online 2320 7876

Research paper UGC CARE Listed (Group -I) Journal Volume 11, Iss 11, Nov 2022

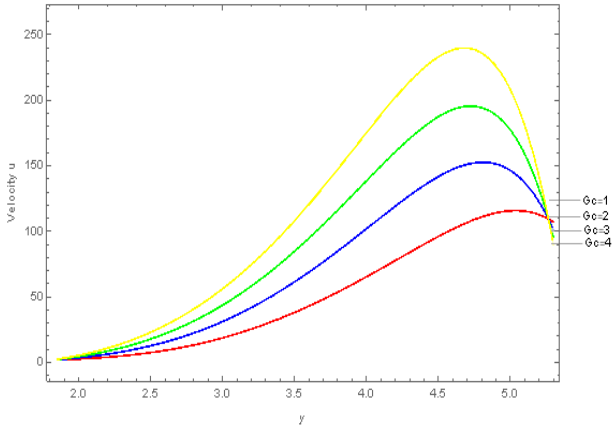

Fig.1 Velocity profile for various values of Gc with M=1, Sc=0.6, Re=1, Pe=0.1, Gr=2, Sr=1, N=2

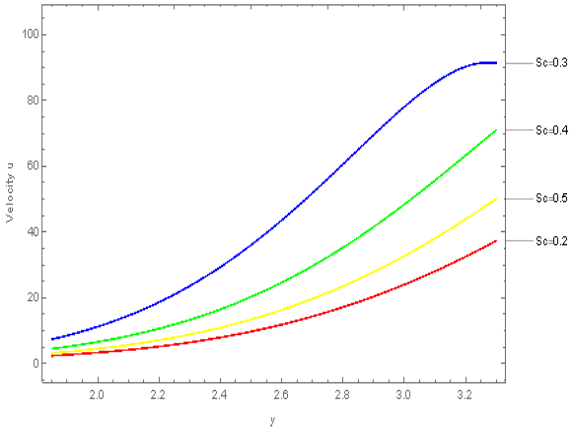

Fig.2 Velocity profile for various values of Sc with M=1, Gc=1, Re=1, Pe=0.1, Gr=2, Sr=1, N=2

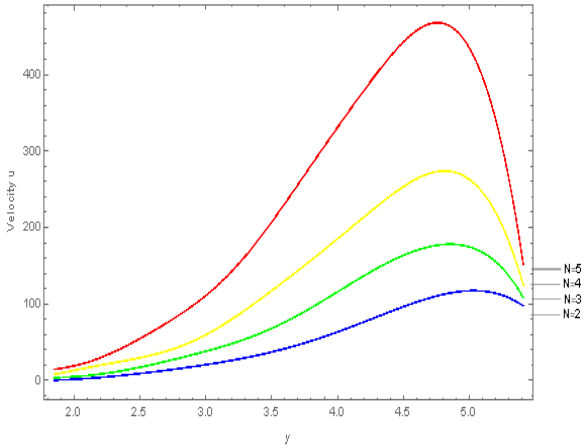

Fig.3 Velocity profile for various values of N with M=1, Gc=1, Re=1, Pe=0.1, Gr=2, Sr=1, Sc=0.6

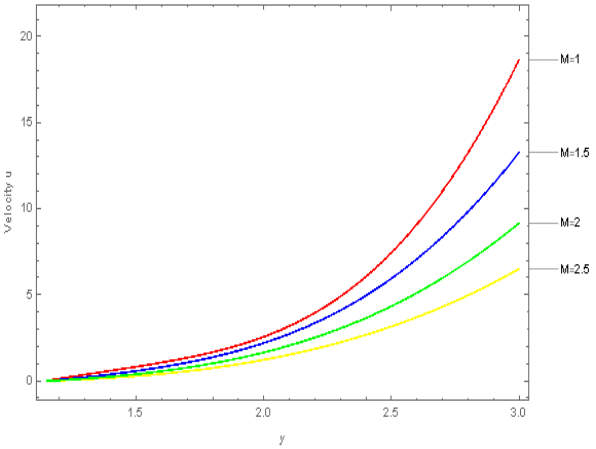

Fig.4 Velocity profile for various values of M with Sc=0.6, Gc=1, Re=1, Pe=0.1, Gr=2, Sr=1, N=2

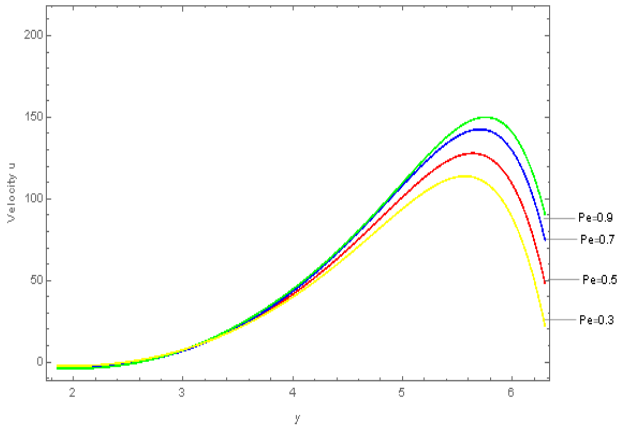

Fig.5 Velocity profile for various values of Pe with M=1, Gc=1, Re=1, Sc=0.6, Gr=2, Sr=1, N=2

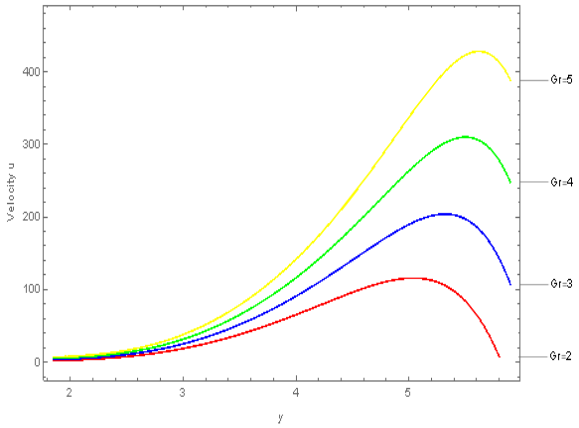

Fig.6 Velocity profile for various values of Gr with M=1, Gc=1, Re=1, Pe=0.1, Sc=0.6, Sr=1, N=2

ISSN PRINT 2319 1775 Online 2320 7876

Research paper UGC CARE Listed (Group -I) Journal Volume 11, Iss 11, Nov 2022

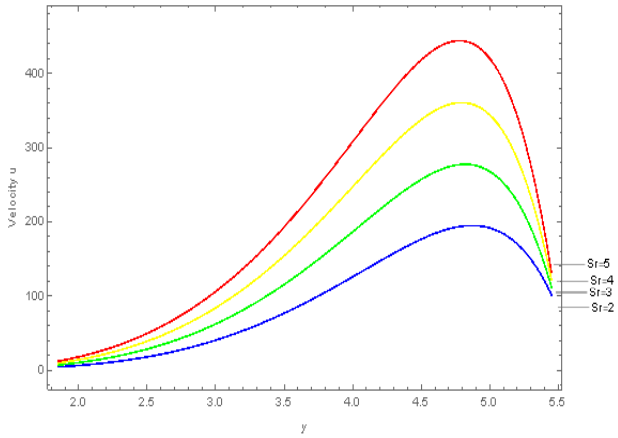

Fig.7 Velocity profile for various values of Sr with M=1, Gc=1, Re=1, Pe=0.1, Gr=2, Sc=0.6, N=2

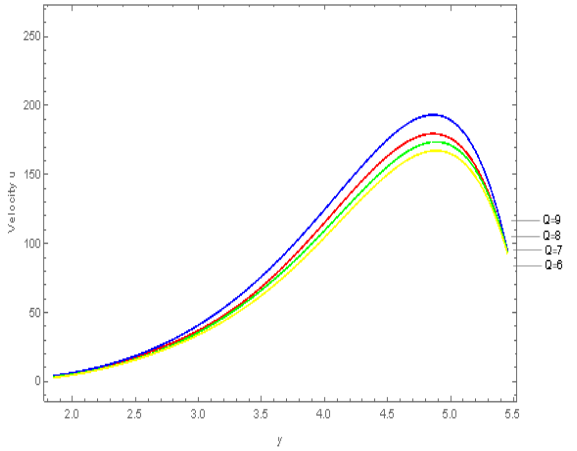

Fig. 8 Velocity profile for various values of Q with M=1, Gc=1, Re=1, Pe=0.1, Gr=2, Sr=1, N=2,Sc=0.6

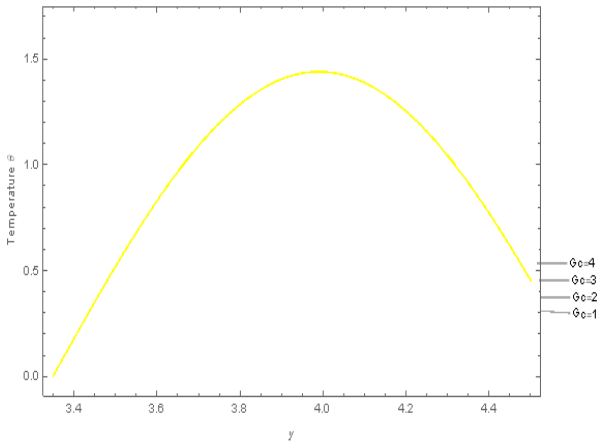

Fig.9 Temperature profile for various values of Gc with M=1,Q=2, Re=1, Pe=0.1, Gr=2, Sr=1,Sc=0.6

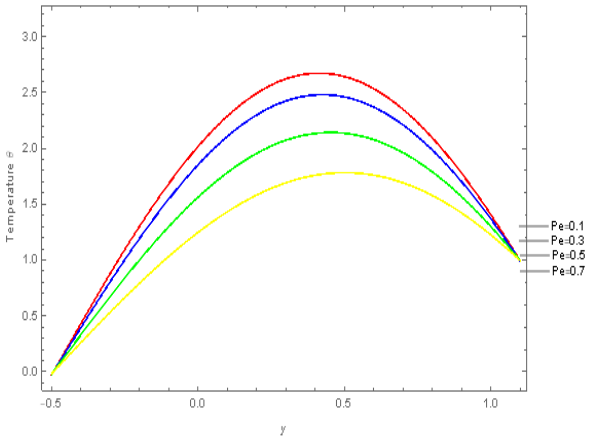

Fig.10 Temperature profile for various values of Pe with M=1, Q=2, Re=1, Gc=1, Gr=2, Sr=1, Sc=0.6

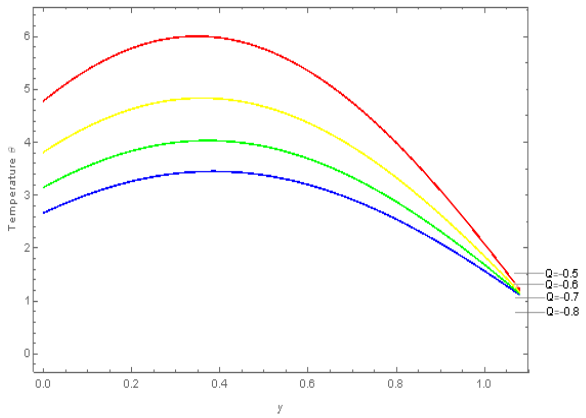

Fig.11 Temperature profile for various values of negative Q with M=1, Pe=0.1, Re=1, Gc=1, Gr=2, Sr=1, N=2,Sc=0.6

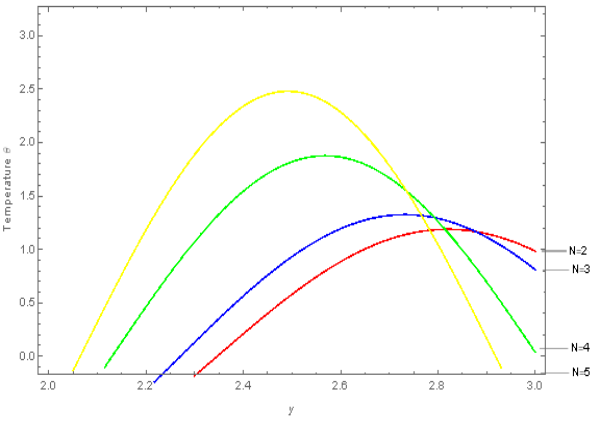

Fig.12 Temperature profile for various values of N with M=1, Pe=0.1, Re=1, Gc=1, Gr=2, Sr=1, Q=2,Sc=0.6

ISSN PRINT 2319 1775 Online 2320 7876

Research paper UGC CARE Listed (Group -I) Journal Volume 11, Iss 11, Nov 2022

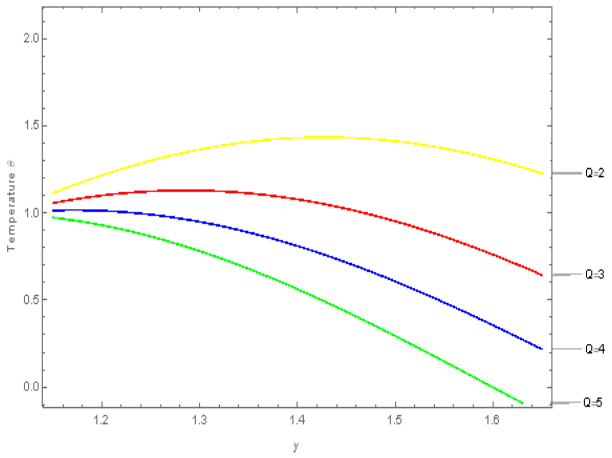

Fig.13 Temperature profile for various values of Q with M=1, Pe=0.1, Re=1, Gc=1, Gr=2, Sr=1, N=2,Sc=0.6

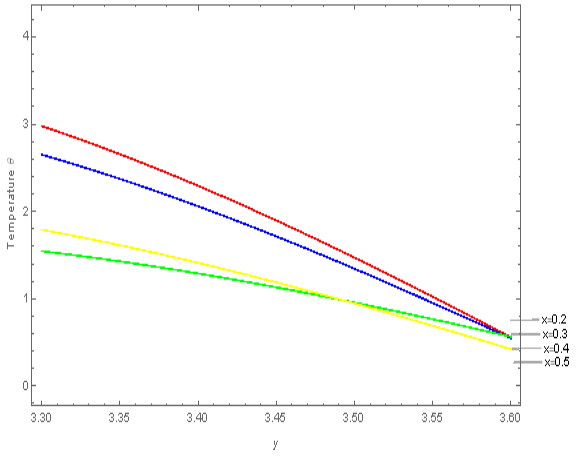

Fig.14 Temperature profile for various values of x with M=1, Pe=0.1, Re=1, Gc=1, Gr=2, Sr=1, N=2, Sc=0.6, Q=2

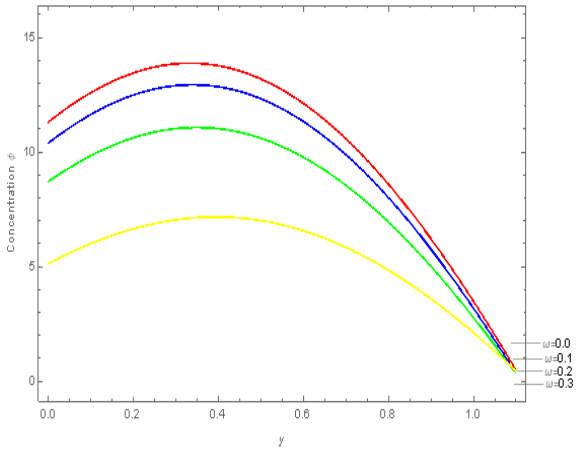

Fig.15 Concentration profile for various values of *w* with M=1, Pe=0.3, Re=1, Gc=1, Gr=2, Sr=1, N=2, Sc=1, Q=2

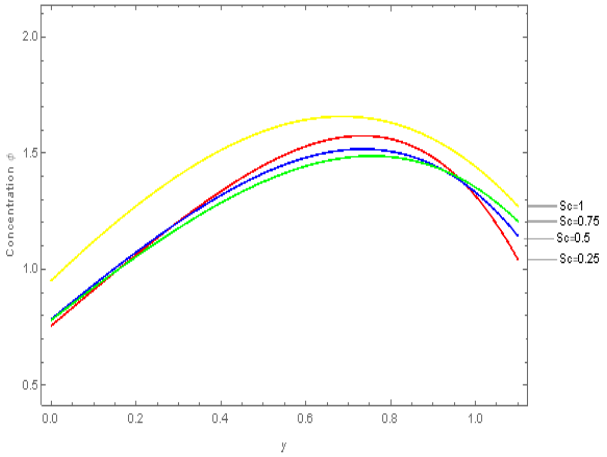

Fig.16 Concentration profile for various values of *Sc* with M=1, Pe=0.3, Re=1, Gc=1, Gr=2, Sr=1, N=2, Q=2

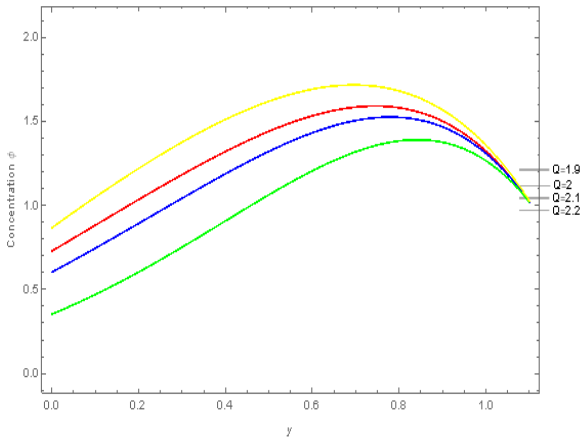

Fig.17 Concentration profile for various values of *Q* with M=1, Pe=0.3, Re=1, Gc=1, Gr=2, Sr=1, N=2,

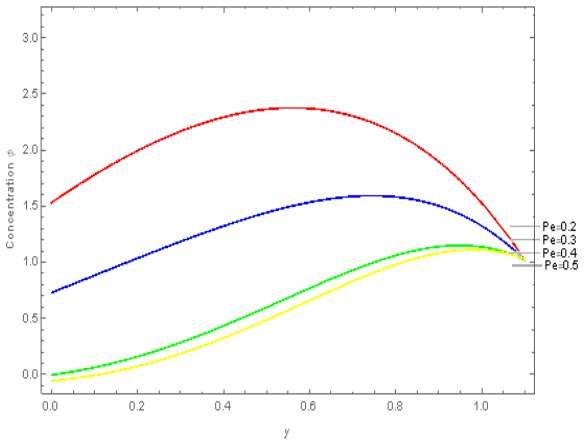

Fig.18 Concentration profile for various values of *Pe* with M=1, Re=1, Gc=1, Gr=2, Sr=1, N=2,

ISSN PRINT 2319 1775 Online 2320 7876

Research paper UGC CARE Listed (Group -I) Journal Volume 11, Iss 11, Nov 2022

Q=2, Sc=0.2

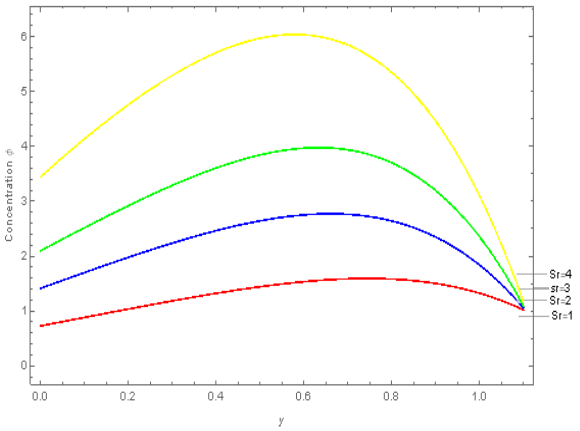

Fig.19 Concentration profile for various values of *Sr* with M=1, Pe=0.3, Re=1, Gc=1, Gr=2, Sr=1, N=2, Q=2, Sc=0.2

Q=2, Sc=0.2

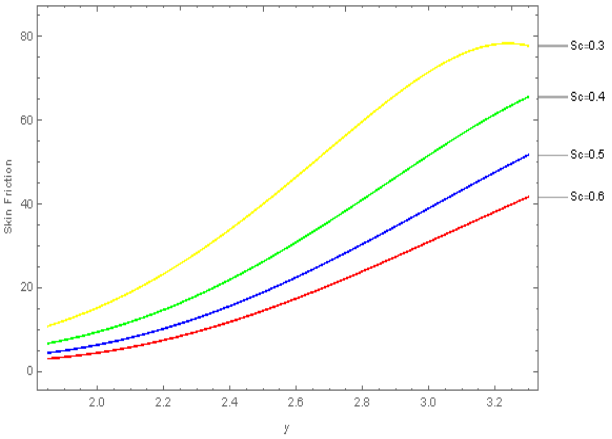

Fig.20 Skin friction for various values of Sc with M=1, Re=1, Gc=1, Gr=2, Pe=0.3, N=2, Q=2, Sr=1

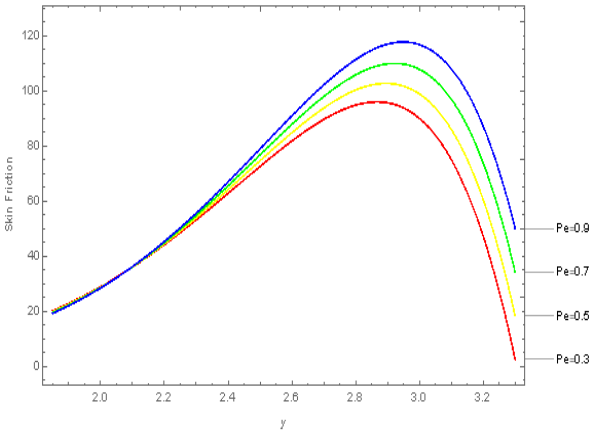

Fig.21 Skin friction for various values of Pe with M=1, Re=1, Gc=1, Gr=2, Sc=0.2, N=2, Q=2, Sr=1

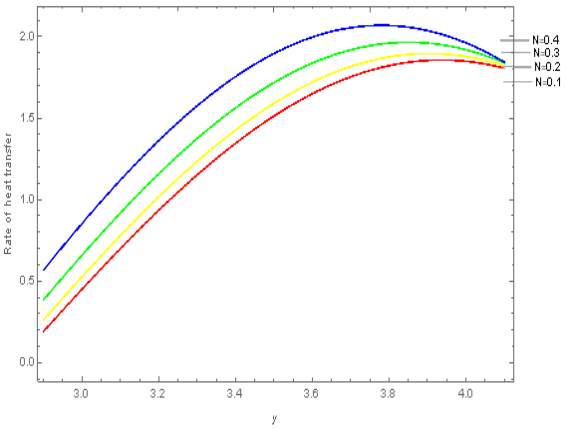

Fig.22 Heat transfer for various values of N with M=1, Re=1, Gc=1, Gr=2, Sc=0.6, Pe=0.1, Q=2, Sr=1

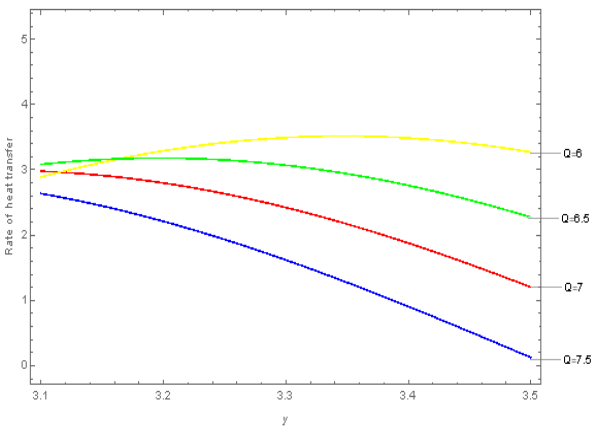

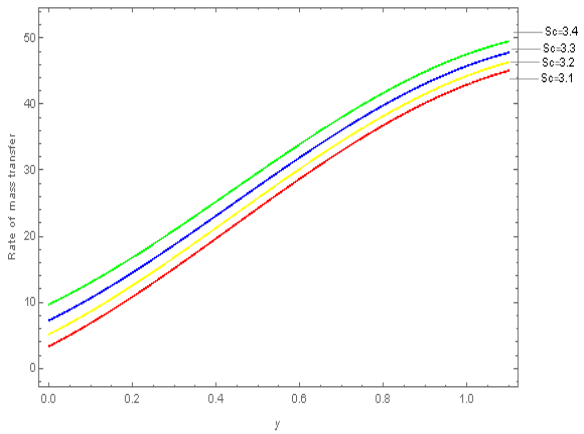

ISSN PRINT 2319 1775 Online 2320 7876

Research paper UGC CARE Listed (Group -I) Journal Volume 11, Iss 11, Nov 2022

Fig.23 Heat transfer for various values of Q with M=1, Re=1, Gc=1, Gr=2, Sc=0.6, Pe=0.1, N=0.1, Sr=1

Fig.24 Mass transfer for various values of Sc with M=1, Re=1, Gc=1, Gr=2,Q=2, Pe=0.2, N=1, Sr=1

Appendix

$$E_1 = \sqrt{N^2 + Q - P_e in}$$

$$E_2 = \sqrt{\frac{K_r + in}{S_c}}$$

$$E_3 = \sqrt{s^2 + M^2 - R_e in}$$

$$A_1 = \left(\frac{1}{S_c E_2^2}\right)\left(\frac{S_c E_2^2 - S_r E_1^2}{e^{E_2 h_1} - e^{2E_2 h_2}}\right)$$

$$A_2 = -A_1 e^{2E_2 h_2}$$

$$A_3 = \frac{\frac{\lambda}{{E_3}^2}\left(e^{E_3(h_2 - h_1)} - 1\right) + \frac{G_r}{{E_3}^2} + \frac{G_c}{{E_3}^2}}{e^{E_3 h_1} - e^{E_3(2h_2 - h_1)}}$$

$$A_4 = \frac{\lambda}{{E_3}^2} e^{E_3 h_2} - A_3 e^{2E_3 h_2}$$

References

[1] Chapman.A.M and Higdon.J.J.L, Oscillatory Stokes flow in periodic porous media, Phys. Fluids, A4, (1992), 2099-2116.

[2] Crittenden.B.D, Lau.A, Brinkmann.T and Field.R.W, Oscillatory flow and axial dispersion in packed beds of spheres, Chem. Eng. Sci., 60, (2005), 111-122.

[3] Dragon.C and Grotberg.J, Oscillatory flow and mass-transport in a flexible tube, J. Fluid Mech., 231, (1991), 135-155.

[4] Graham.D.R and Higdon.J.J.L, Oscillatory forcing of flow through porous media. Part 1. Steady flow, J. Fluid. Mech., 465, (2002), 213-235.

[5] Loganathan.C and Prathiba.S.R, Magnetohydrodynamic flow past a porous spherical aggregate with stress jump condition, Progress in Nonlinear Dynamics and Chaos, 1, (2013), 76-92.

[6] Loganathan.C and Prathiba.S.R, Magnetohydrodynamic oscillatory Stokes flow past a porous sphere, Elixir Applied Mathematics, 74, (2014), 26960-26974.

[7] Looker.J.R and Carnie.S.L, The hydrodynamics of an oscillating porous sphere, Phys. Fluids, 16, (2004), 62-72.

[8] Prathiba.S.R and Sumathi.K, Magnetohydrodynamic flow past a rotating circular cylinder, International Journal of Computer Application, 4(3), (2013), 18-29.

[9] Sasikumar.J, Govindarajan.A, Soret effect on chemically radiating MHD oscillatory channel with heat source through porous medium in asymmetric wavy channel, Journal of Physics: Conference Series, 1000, (2018), 012034.

[10] Satya Narayana.P.V, Venkateswarlu.B and Devika.B, Chemical reaction and heat source effects on MHD oscillatory flow in an irregular channel, Ain shams Engineering Journal, 7 (4), (2015), 1079-1088.

ISSN PRINT 2319 1775 Online 2320 7876

Research paper UGC CARE Listed (Group -I) Journal Volume 11, Iss 11, Nov 2022

[11] Sudharsan Reddy, Manjulatha.V, Vijaykumar Varma.S and Raju.V.C.C, Effects of radiation and chemical reaction on the MHD oscillatory flow in an asymmetric wavy channel, Advances and Applications in fluid Mechanics, 17 (1), (2014), 39-60.

[12] Wang.C.C and Chen.C.K, Forced convection in a wavy wall channel, International Journal of Heat and Mass Transfer, 45 (12), (2002), 2587-2595.